

## Activated Carbon Production from Peat Using ZnCl<sub>2</sub>: Characterization and Applications

Toni Varila,<sup>b</sup> Davide Bergna,<sup>a,b</sup> Riikka Lahti,<sup>a,b</sup> Henrik Romar,<sup>a,b,\*</sup> Tao Hu,<sup>a</sup> and Ulla Lassi<sup>a,b</sup>

The process for producing activated carbon from peat was optimized. The peat was impregnated with different ratios of ZnCl<sub>2</sub>, and the impregnated biomass was activated at different temperatures. The specific surface area, pore size distribution, total carbon content, and yield of the activated carbon were investigated. The best results for the specific surface area and mesoporosity of the activated peat were obtained by using a high impregnation ratio (2) and high activation temperature (1073 K). Highly porous activated carbon was produced that had a specific surface area of approximately 1000 m<sup>2</sup>/g and total pore volume that was higher than 0.5 cm<sup>3</sup>/g for most samples. The activated carbon had a high degree of mesoporosity. The adsorptive properties of the activated carbon were determined with methylene blue and orange II dyes.

*Keywords:* Peat; Zinc chloride; Activation; Activated carbon; Mesoporous carbon; Optimization

*Contact information:* a: University of Oulu, Research Unit of Sustainable Chemistry, P.O. Box 3000, FI-90014 University of Oulu, Finland; b: University of Jyväskylä, Kokkola University Consortium Chydenius, Applied Chemistry, P.O. Box 567, FI-67101 Kokkola; \*Corresponding author: henrik.romar@chydenius.fi

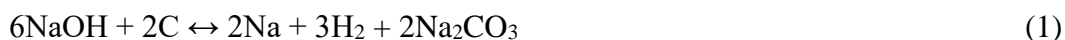
### INTRODUCTION

Over the last few decades, the preparation of activated carbon with the desired chemical and physical properties has gained a lot of interest (Marsh and Rodríguez-Reinoso 2006). A highly porous structure and high specific surface area are features of activated carbon that are widely desired in many purification applications in industrial and municipal processes. Wastewater treatment, gas cleaning processes, metal removal from waste streams, and usage as a catalyst are the main applications for activated carbon (Patrick 1995; Ahmadpour and Do 1996; Cox *et al.* 2005; Mohammad-Khah and Ansari 2009; Caglayan and Aksoylu 2013; Fu and Li 2015). Recently developed applications of activated carbon include electrical charge storage (*i.e.*, super capacitors) and gas storage (*i.e.*, hydrogen) (Li *et al.* 2016). However, the high cost of activated carbon limits its applications in many cases (Özdemir *et al.* 2011). For this reason, low-cost and renewable starting materials are widely used to produce activated carbon. Biomass-based activated carbon can be prepared from a number of carbon rich biomasses, such as coconut shell, coal, saw dust, and peat (Ahmedna *et al.* 2000; Antal and Grønli 2003; Mohammad-Khah and Ansari 2009; Khadiran *et al.* 2015). Peat is commonly used as a raw material for energy and heat production, especially in Finland. This is mainly because the peat, as a raw material, is relatively cheap and has been considered as a renewable energy resource. By a decision of the European Union in 2008, peat is no longer regarded as a renewable energy resource. Recently in Finland, the usage of peat to produce activated carbon has gained some interest among researchers and companies in order to find new applications for the peat.

There are two well-known methods for producing activated carbon, which are physical activation and chemical activation. Physical activation is performed in a two-step process. First, the biomass is placed in a reactor flushed continuously with a nitrogen atmosphere in order to avoid total oxidation. Heat is then fed into the system, which results in the carbonization of the biomass at temperatures near 673 K. The carbonization temperature is one of the most important parameters that affects the physical properties of the activated carbon. Generally, peat contains cellulose, hemicellulose, lignin, ash, and other organic compounds. The carbonization process is needed in order to decompose these organic compounds into activated carbon. The properties of the activated carbon vary according to the temperature used. The carbonized biomass is activated by a partial oxidant agent, such as steam or carbon dioxide, at high temperatures (873 to 1073K) (Hanna *et al.* 2015). Activating agents are responsible for the creation of the pore structure.

The advantages of physical activation are the relative simplicity and low cost, while the disadvantage is low yields (Lillo-Ródenas *et al.* 2003; Yorgun *et al.* 2009). For example, more volatile compounds are formed at higher carbonization temperatures, while decomposed organic compounds exit the carbonization process, which leads to lower yield of activated carbon. Furthermore, the holding time effects the yield of activated carbon in the same way as the carbonization temperature. The longer the holding period is, the more time organic compounds have to decompose (Baçaoui *et al.* 2001; Lua and Yang 2004; Yang *et al.* 2010).

In addition to physical activation, chemical agents, *e.g.*, zinc chloride ( $\text{ZnCl}_2$ ), KOH, NaOH, and  $\text{H}_3\text{PO}_4$ , can be used for activating carbon (Lillo-Ródenas *et al.* 2003; Yorgun *et al.* 2009). In the chemical activation process, the biomass is first impregnated with a solution containing the chemical activating agent, dried in an oven, and then heated in a furnace, with rather lower temperatures (673 to 873 K) compared to physical activation, under an inert atmosphere (nitrogen atmosphere). In the case of chemical activation, important factors include the correct mass to carbon ratio to avoid excessive consumption of reagents and proper activation temperature, which can vary according to the type of chemical agent used. From the mechanical point of view, chemical reactions that occur during the carbonization process are not well known. Only few studies have reported about how the chemical activation occurs. In the case of hydroxides (NaOH and KOH), the reactions between carbon and alkaline metals produces metal, hydrogen and metal carbonates. The following reaction can be described with equations 1 and 2 (Lillo-Ródenas *et al.* 2004).



However, there is a lack of information about how the reaction between carbon and  $\text{ZnCl}_2$  or  $\text{H}_3\text{PO}_4$  occur during the carbonization process. Only assumptions can be made at this point. Further investigation is needed in this field.

The typical advantages of using chemical activation include the possibility of achieving higher final carbon yields, the fact that it can be a one step process, the generally lower activation temperatures that are required, and an easier adjustment of porosity compared with physical activation (Hayashi *et al.* 1995; Ahmadpour and Do 1996; Benaddi *et al.* 1998; Yorgun *et al.* 2009; Yorgun and Yıldız 2015). The main disadvantages of using chemical compounds are that they are not environmentally friendly substances and are corrosive towards the equipment used during research. An acid washing step is also needed

in order to remove the chemical activating agent (Teng and Lin 1998; Yorgun *et al.* 2009; Yorgun and Yıldız 2015).

A large specific surface area, well-developed highly porous structure, stability, and surface chemical functional groups are key factors of activated carbon. The adsorption of dyes with large diameters can be used to determine the possible pore structure and interaction mechanisms of activated carbon. Methylene blue and orange II are commonly used dyes. Methylene blue is a basic (cationic) dye, while orange II is an acidic (anionic) dye. The adsorption of dyes is favored by mesoporous (2 to 50 nm) carbon because the molecular size of the dyes is larger than the micropores. In addition to the diffusion into pores, the dye molecules can interact with the surface charge of the activated carbon (Rodríguez *et al.* 2009; Peng *et al.* 2014; Kumar and Jena 2016a). In this work the above-mentioned dyes were used to measure the adsorption ability of peat based activated carbons.

The aim of this study was to optimize the chemical activation process using  $ZnCl_2$  in order to produce highly mesoporous activated carbon with a pore size distribution suitable for use as a catalyst support and adsorption of larger organic molecules. The effect of the activation temperature and different impregnation ratios of peat and  $ZnCl_2$  on the specific surface area, pore size distribution, yield, total carbon (TC), and adsorption abilities of the peat-based activated carbon were investigated. The term “impregnation ratio” describes the ratio of mass of  $ZnCl_2$  to the dry mass of peat.

## MATERIALS AND METHODS

### Biomass and Materials

The peat used in this experiment was obtained from peatlands in the Oulu region of northern Finland. The peat was initially washed with distilled water to remove any impurities, such as metals, and then oven dried at 393 K for 24 h. The peat was then sieved so that a fraction 0.5 to 1 mm in size was collected. The resulting fraction was used for further experiments. All reagents used in this research were ordered from VWR International (Helsinki, Finland).

### Moisture, Ash Content, and Elemental Analyses of the Peat

The moisture content and ash content of the peat was measured by using the standard test methods for peat (ASTM D 2974-87). A known amount of peat was weighed in a tared crucible. The crucible was dried overnight in an oven at 378 K. The dried sample was placed in a desiccator and allowed to cool down to room temperature. The crucible was weighed, and the moisture content was calculated by dividing the weight loss by the initial weight of the sample. The crucibles with dried peat was used for determination of the ash content. Organic matter was totally carbonized and removed in a furnace at 713 K for 3 h. The sample was allowed to cool down in a desiccator to room temperature before weighing it. Ash content was calculated as the mass ash as percent of the initial mass. Elemental analysis of the peat was performed with a Flash 2000 analyzer (ThermoScientific, Waltham, MA, USA). Ground elements were converted into simple gases ( $CO_2$ ,  $H_2O$ ,  $N_2$ , and  $SO_2$ ) in an oxygen atmosphere and detected with a TDC detector.

## Preparation, Chemical Activation, and Carbonization of the Peat-Based Activated Carbons

Four series, each containing different impregnation ratios of ZnCl<sub>2</sub> to peat, were prepared according to the method described in Liu (2010). The impregnated peat was dried and carbonized at different temperatures, which are given in Table 1. Each peat sample (P) was named according to the carbonization temperature and ZnCl<sub>2</sub> to peat ratio used. The samples were prepared by adding a known amount of peat and zinc chloride solution to an 800-mL beaker. Under mechanical stirring, the prepared solution was heated to 358 K for 3 h in order to complete the chemical impregnation. Deionized water was added into the solution at various time intervals to prevent it from completely drying out. The impregnated biomass was then dried at 378 K for 24 h in an oven with natural convection.

The impregnated peat samples were crushed in a mortar and activated in a stainless-steel fixed-bed reactor. The reactor was placed in a tubular heating oven for carbonization. During the heating process, the reactor was flushed with an inert gas (nitrogen) in order to avoid oxidation. The oven temperature was increased from room temperature to the final temperatures, which are shown in Table 1, using a heating ramp of 10 K/min and hold time of 2 h at the final carbonization and activation temperature. To obtain the final activated carbon, the chemical activating agent remaining in the sample after carbonization was removed by refluxing the sample with 3 M HCl for 1 h. The carbon was filtered and washed with distilled water until a neutral filtrate was obtained. The activated carbon was finally oven-dried overnight at 378 K (Yorgun *et al.* 2009).

**Table 1.** Preparation Method of the Activated Carbons

Sample	Impregnation ratio	Activation Temperature (K)
P <sub>2_723</sub>	2	723
P <sub>2_773</sub>	2	773
P <sub>2_873</sub>	2	873
P <sub>2_1073</sub>	2	1073
P <sub>1_723</sub>	1	723
P <sub>1_773</sub>	1	773
P <sub>1_873</sub>	1	873
P <sub>1/2_723</sub>	1/2	723
P <sub>1/2_773</sub>	1/2	773
P <sub>1/2_873</sub>	1/2	873
P <sub>1/4_723</sub>	1/4	723
P <sub>1/4_773</sub>	1/4	773
P <sub>1/4_873</sub>	1/4	873

### Calculation of the Yield and Total Carbon (TC)

The yield of activated carbon for each sample was calculated from the weight of the resultant peat-based activated carbon divided by the weight of the initial sample used for carbonization and activation (Yorgun *et al.* 2009). The content of carbon present in each sample, given as the TC percent, was measured using a solid phase carbon analyzer (Skalar Primacs MCS, Breda, The Netherlands). The dried and crushed samples were weighed in quartz crucibles, combusted at 1373 K in an atmosphere of pure oxygen, and the resulting CO<sub>2</sub> was analyzed by an IR analyzer (Skalar Formacs, Skalar, Breda, The Netherlands). The carbon content values were obtained by comparing the signal from the IR analyzer with a calibration curve derived from known masses of a standard substance (citric acid). The total mass of carbon in each sample was calculated as a percent of the

mass initially weighed, and was only determined in the final product, which was carbonized, chemically activated, and acid washed.

### Specific Surface Area and Pore Size Distribution

Prior to measurement, portions of each sample (approximately 200 mg) were pretreated at low pressures and high temperatures in order to clean the surfaces. Isothermal conditions were obtained by immersing the sample tubes in liquid nitrogen (76 K). Nitrogen was then added to the samples in small steps, and the adsorption isotherms were obtained. The specific surface areas were calculated from the adsorption isotherms according to the Brunauer–Emmett–Teller (BET) method (Brunauer *et al.* 1938). The pore size distributions were calculated using the Barrett-Joyner-Halenda (BJH) algorithm (Barrett *et al.* 1951). With a Micromeritics ASAP 2020 (Norcross, USA), pores down to 1.5 nm in diameter could be measured.

### Field Emission Scanning Electron Microscope (FESEM) and Transmission Electron Microscope (TEM) Imaging

A field emission scanning electron microscope (FESEM) (Zeiss Sigma, Jena, Germany) equipped with an energy-dispersive X-ray spectrometer (EDS) and Electro Backscatter Diffraction (EBSD) camera, located in the Center of Microscopy and Nanotechnology, University of Oulu, was used to study the microstructure of the peat samples. Scanning electron microscope (SEM) images were taken with an acceleration voltage of 5 kV and working distance of approximately 5 mm without any coating. High-resolution transmission electron microscope (TEM) images were taken with a JEOL JEM-2200FS TEM (Tokyo, Japan) at an acceleration voltage of 200 kV.

### Adsorptive Properties

The adsorptive properties of the peat-based activated carbon were tested using the adsorption of dyes, methylene blue (MB) and orange II (OII), into the pores, as previously described (Hirata *et al.* 2002; Raposo *et al.* 2009). A solution containing 300 mg of MB or OII per liter of H<sub>2</sub>O was prepared, and 100 mL of this solution was then transferred into 250-mL Erlenmeyer flasks. Fifty milligrams of activated carbon were added next, and the solutions were continuously agitated for 24 h to achieve equilibrium between adsorption and desorption of the test dye. Portions of each solution were filtered and diluted if needed. The absorbance of the solution was measured at 664 nm for MB and at 485 nm for OII on a Shimadzu UV-1700 double-beam spectrophotometer (Kyoto, Japan). The concentrations of the solution was calculated from calibration lines obtained with known concentrations of MB and OII respectively. The absorbed mass ( $q_{abs}$ ) was calculated for each compound using Eq. 6, and the percent MB and OII removed was calculated using Eq. 7,

$$q_{abs} = ((C_0 - C_t) \times V) / m \quad (6)$$

$$\% \text{ removed} = (C_0 - C_t) / C_0 \quad (7)$$

where  $C_0$  is the initial concentration of the dye (300 mg/L),  $C_t$  is the measured concentration (mg/L) after 24 h,  $V$  is the volume of dye solution used (L), and  $m$  is the mass of the activated carbon used (mg). In this work, the kinetics of MB and OII adsorption were not considered.

## RESULTS AND DISCUSSION

### Peat Analysis

As mentioned earlier in material and methods part, the physical properties of peat obtained from northern part of Finland were investigated. Data obtained from the moisture, ash content, and elemental analysis tests are presented in Fig. 1.

According to the results peat is mostly consisting of carbon-containing materials, especially lignin, cellulose, and hemicellulose, 54% on a wet basis. Water content (34%) is also very high compared to carbon content. Elemental analysis of peat showed that nitrogen (1%), sulfur (2%), and hydrogen (6%) content were relatively small compared to carbon and water content. The remaining 3%, ash content, consist mostly of metals or their oxides.

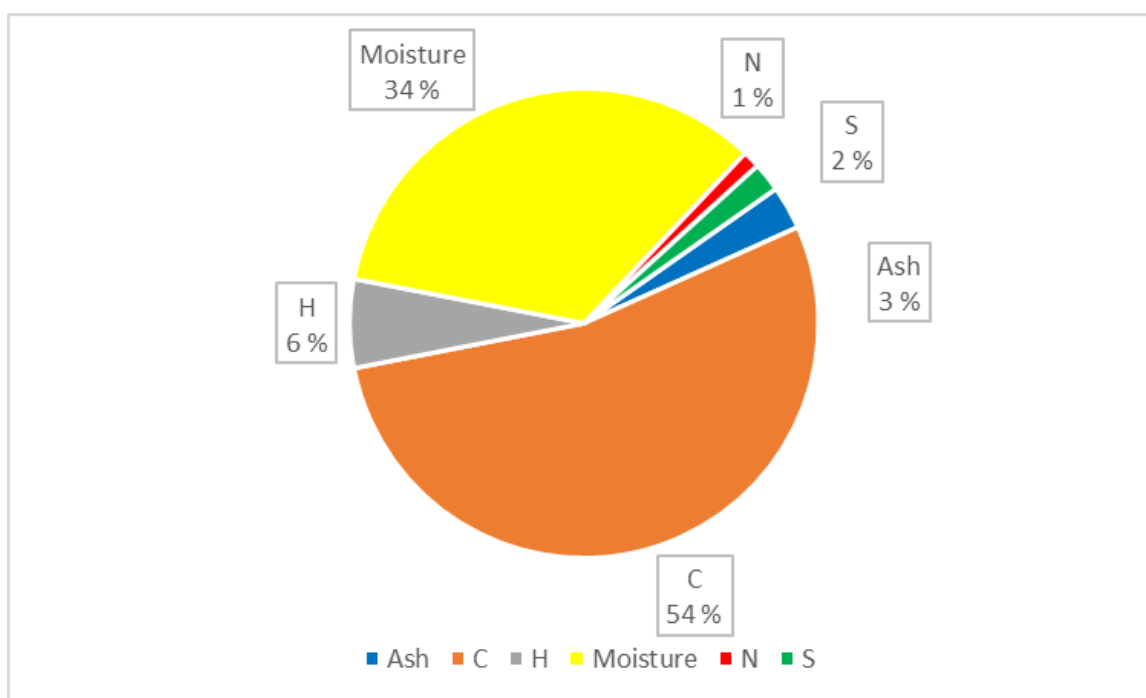


Fig. 1. Results from the moisture, ash content, and elemental analyses of the raw peat sample

### Effect of the Carbonization Temperature on the Activated Carbon Yield and Total Carbon of the Activated carbon

The effect of the carbonization temperature, which ranged from 723 to 1073 K, on the total yield and TC was investigated. The results are shown in Table 2. According to the results, the yield decreased from 45.7% to 14.2% when the carbonizing temperature increased from 723 to 1073 K. This finding was in line with earlier studies (Baçaoui *et al.* 2001; Lua and Yang 2004; Ozdemir *et al.* 2014).

Higher TC values were obtained when using high carbonization temperatures. More volatile compounds were formed, which increased the TC content (measured as % TC) but decreased the total mass of the activated carbons. Stimely and Blankenhorn (1985) obtained the same results while investigating the behavior of different wood species treated at different temperatures.

**Table 2.** Effect of the Carbonization Temperature and Impregnation Ratio on the Yield and Total Carbon Content of the Activated Peat Samples

Sample	TC (%)	Yield (%)
P <sub>2_723</sub>	87.2	43.7
P <sub>2_773</sub>	88.3	43.1
P <sub>2_873</sub>	90.3	39.8
P <sub>2_1073</sub>	96.0	14.2
P <sub>1_723</sub>	73.3	40.8
P <sub>1_773</sub>	89.3	40.3
P <sub>1_873</sub>	90.4	40.0
P <sub>½_723</sub>	89.3	40.5
P <sub>½_773</sub>	85.6	42.2
P <sub>½_873</sub>	92.5	38.6
P <sub>¼_723</sub>	76.5	45.7
P <sub>¼_773</sub>	72.3	44.0
P <sub>¼_873</sub>	80.9	42.4

### Effect of the Impregnation Ratio on the Yield and Total Carbon content of the Activated Carbons

The effect of the impregnation ratio on the TC and yield of peat-based activated carbon was also investigated. According to the results, which are shown in Table 2, there was a slight correlation between the impregnation ratio and yield. Increasing the impregnation ratio from ¼ to 2 at any temperature lowered the overall yield by a few percentage points. At low concentrations, ZnCl<sub>2</sub> reacts with H and O on the surface of the peat and forms H<sub>2</sub>O and H<sub>2</sub>, rather than burning away the carbon (CO and CO<sub>2</sub>), which leads to higher yields, as shown by Liu *et al.* (2016) and Qian *et al.* (2007).

### Effect of the Carbonization Temperature and Impregnation Ratio on the Specific Surface Area and Pore Size Distribution of the Peat-Based Activated Carbons

The isotherms of the activated peat samples are presented in Fig. 2. The specific surface area and pore size distribution were determined at different activation temperatures (723 to 1073 K) and ZnCl<sub>2</sub> impregnation ratios (¼ to 2).

According to the data obtained and presented in Table 3, increasing the temperature from 723 to 1073 K resulted in higher specific surface areas, which was independent of the impregnation ratio. Increasing the carbonization temperature accelerates the volatilization and decomposition of the sample, which leads to an increase in the specific surface area and enhanced pore development (Yorgun and Yıldız 2015).

High impregnation ratios and a high temperature (1073 K) led to a lower surface area and pore volume. The specific surface area and pore volume of the samples that had an impregnation ratio of 2 decreased from 923 to 790 m<sup>2</sup>/g and from 0.78 to 0.50 cm<sup>3</sup>/g, respectively, when the carbonization temperature was increased from 873 to 1073 K. The boiling point of ZnCl<sub>2</sub> is 732 K, and at 1073 K, melted ZnCl<sub>2</sub> expands existing micropores into mesopores. This process leads to a lower overall specific surface area and pore volume (Demiral *et al.* 2008; Bouchemal *et al.* 2009). The pore size distribution in all of the peat samples were mainly in the mesoporous region. Increasing the impregnation ratio from ¼ to 1 rapidly increased the specific surface area and pore volume of the activated peat samples. The specific surface area and pore volume for P<sub>¼\_873</sub> were 341 m<sup>2</sup>/g and 0.16 cm<sup>3</sup>/g, respectively, and for P<sub>1\_873</sub> were 1361 m<sup>2</sup>/g and 0.69 cm<sup>3</sup>/g, respectively.

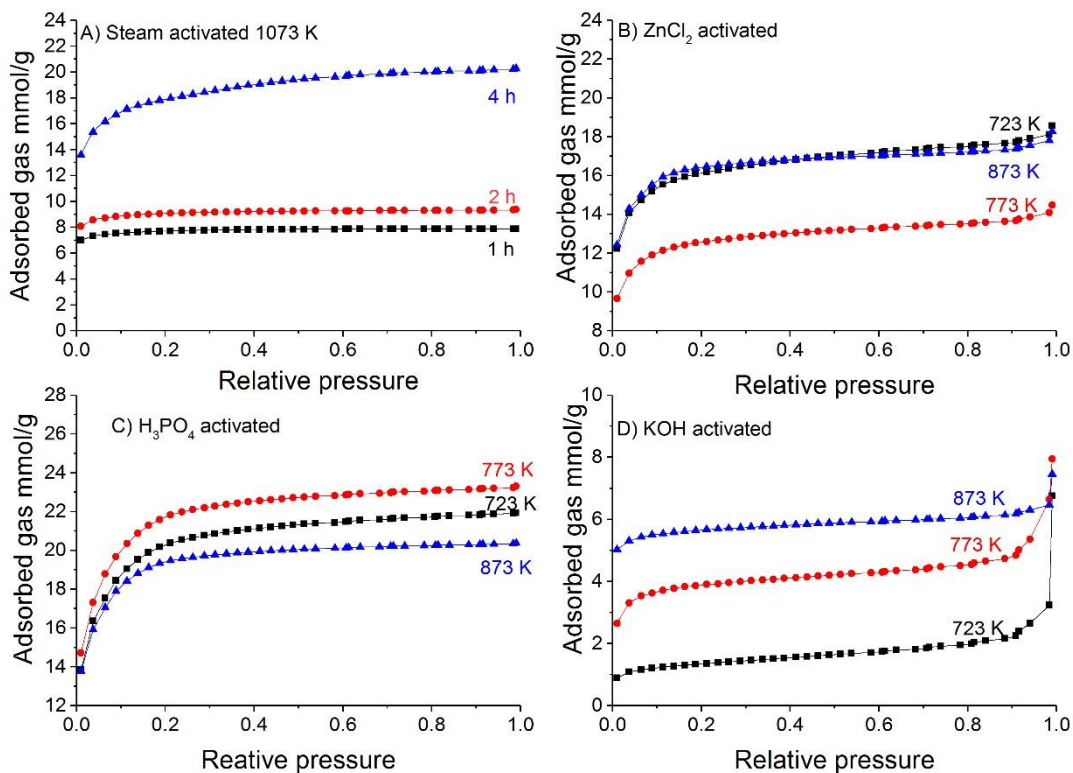


**Fig. 1.** Adsorption isotherms for peat activated at different temperatures using different impregnation ratios: a) 1:1 impregnation ratio; b) 1:2 impregnation ratio; c) 1:4 impregnation ratio; d) 2:1 impregnation ratio

**Table 3.** Effect of the Impregnation Ratio and Temperature on the Specific Surface Area (SSA) and Pore Size Distribution of the Activated Peat Samples

Sample	Impregnation Ratio	Temperature (K)	SSA (m <sup>2</sup> /g)	Pore Volume (cm <sup>3</sup> /g)	Micro pores (%)	Meso pores (%)	Macro pores (%)
P <sub>2_723</sub>	2	723	511	0.29	32.7	65.7	1.7
P <sub>2_773</sub>	2	773	731	0.51	20.2	78.7	1.1
P <sub>2_873</sub>	2	873	923	0.78	14.9	84.2	0.9
P <sub>2_1073</sub>	2	1073	790	0.59	18.8	80.2	1.0
P <sub>1_723</sub>	1	723	946	0.76	19.9	79.1	0.9
P <sub>1_773</sub>	1	773	1081	0.57	40.9	58.1	1.1
P <sub>1_873</sub>	1	873	1361	0.69	46.7	52.4	0.9
P <sub>½_723</sub>	1/2	723	1224	0.66	40.6	58.6	0.8
P <sub>½_773</sub>	1/2	773	960	0.43	44.1	53.9	2.0
P <sub>½_873</sub>	1/2	873	1130	0.50	47.1	50.8	2.1
P <sub>¼_723</sub>	1/4	723	75	0.04	24.5	65.5	10.0
P <sub>¼_773</sub>	1/4	773	271	0.13	36.5	57.9	5.7
P <sub>¼_873</sub>	1/4	873	341	0.16	35.7	58.1	6.2

The impregnation ratio also had an effect on the pore size distribution. The microporosity decreased when the impregnation ratio increased. In contrast, the mesoporosity increased when the impregnation ratio increased. Other research groups have also come to the same conclusions concerning the effects of the carbonization temperature



and chemical activating agent ratio on the specific surface area and pore size distribution (Yang and Qiu 2011; Kumar and Jena 2015; Kumar and Jena 2016b).

### Adsorption Tests

The adsorptive properties of the activated carbon were tested using MB and OII adsorption tests. The results of the tests are presented in Table 4 and Fig. 3.

**Table 4.** Adsorption Ability of the Activated Peat Samples

Sample	MB Adsorption (%)	MB Adsorption (mg/g)	OII Adsorption (%)	OII Adsorption (mg/g)
P <sub>2_723</sub>	35	111	46	147
P <sub>2_773</sub>	49	157	76	241
P <sub>2_873</sub>	63	200	87	275
P <sub>2_1073</sub>	67	212	83	263
P <sub>1_723</sub>	66	209	83	264
P <sub>1_773</sub>	54	172	83	264
P <sub>1_873</sub>	74	233	93	253
P <sub>½_723</sub>	70	221	95	300
P <sub>½_773</sub>	54	171	52	164
P <sub>½_873</sub>	77	244	86	273
P <sub>¼_723</sub>	2	6	6	18
P <sub>¼_773</sub>	5	17	7	21
P <sub>¼_873</sub>	5	17	9	28

MB: Methylene blue; OII: Orange II

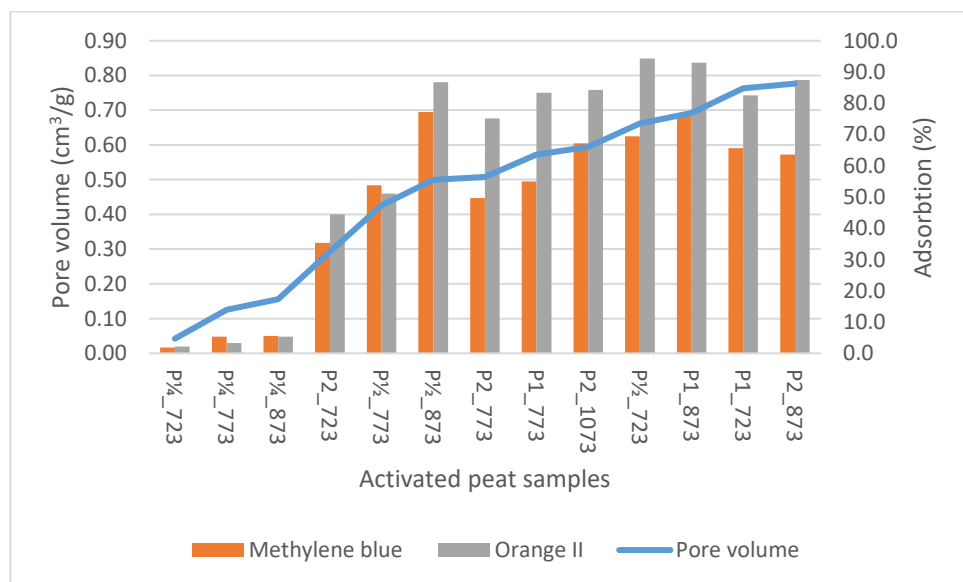


**Fig. 2.** Effect of the pore volume on the adsorption ability. The samples are in order of increasing pore volume.

The percentage of dye adsorbed increased with an increasing pore volume. A pore volume of at least 0.3 cm<sup>3</sup>/g was necessary for any adsorption to occur. The removal of the acidic OII dye was more efficient than the removal of the basic MB dye. The maximum removal of OII was 95% (300 mg/g) for sample P<sub>½\_723</sub>, and the maximum removal of MB was 77% (244 mg/g) for sample P<sub>½\_873</sub>. In addition to the pore volume, the surface groups

on the activated carbon might affect the adsorption. Because the removal of the anionic dye (OII) was more efficient than the removal of the cationic dye (MB), there might have been more positively charged functional groups on the activated carbon surface than negatively charged groups. Earlier Ma *et al.* (2015) reported contradictory findings while investigating the adsorption abilities, with methylene blue and orange II, of the activated carbon produced from banana peels.

### Scanning Electron Microscope (SEM) and Transmission Electron Microscope (TEM) Images

The surface structure of the activated peat samples was studied by scanning electron microscopy. Four activated peat samples with different impregnation ratios activated at the same temperature are presented in Fig. 4. According to the SEM images, large pores can clearly be seen on the surface of all of the samples, regardless of the impregnation ratio. These pores can be regarded as transportation pores into the porous systems created by the activation processes even if the meso- and microporous structures are impossible to be visualized at the magnification levels used. Furthermore, a fine porous structure could be observed at the edge or cross-section of the particles using a high magnification (data not shown).

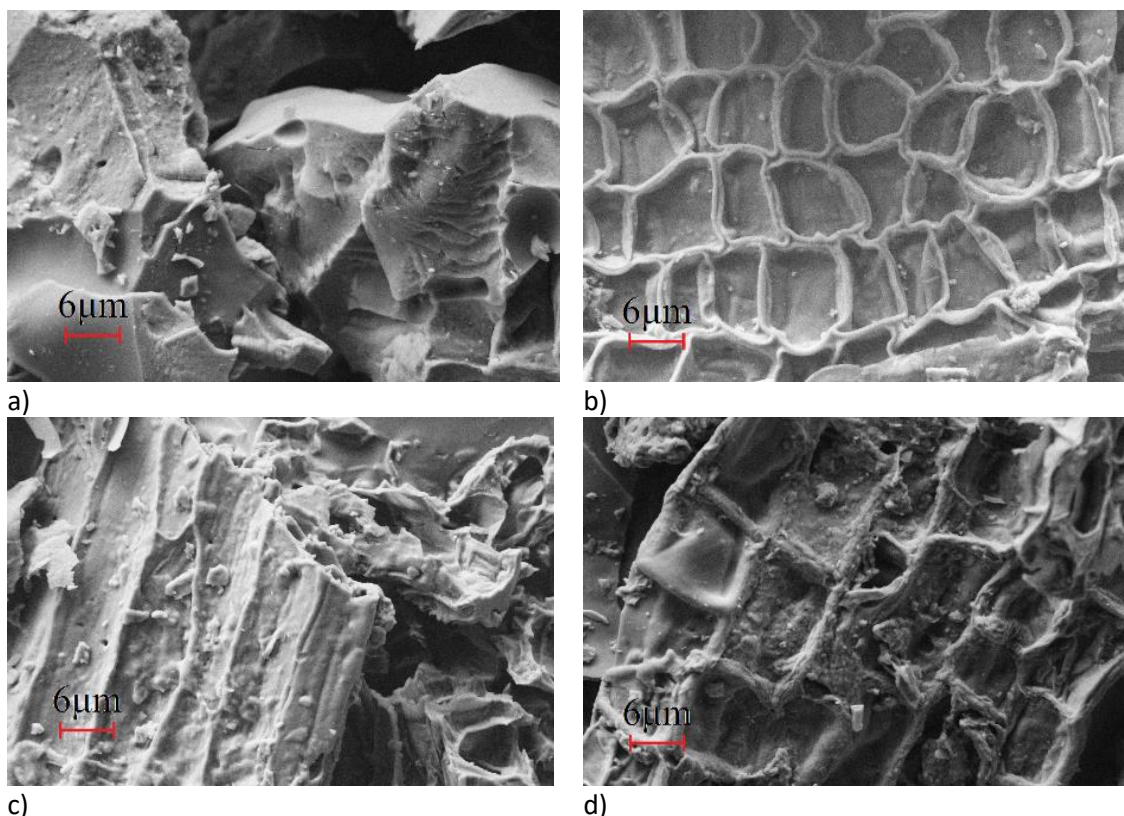


**Fig. 3.** SEM images of the activated peat samples. The magnification in the images is 5000 X; a) P<sub>2\_873</sub>; b) P<sub>1\_873</sub>; c) P<sub>½\_873</sub>; d) P<sub>¼\_873</sub>

The TEM images of these four peat samples (Fig. 5) showed they had similar structures. All four peat samples had an amorphous structure that is typical of carbon black. According to Fig 5 no remaining metal can be found indicating that the process for metal removal is complete.

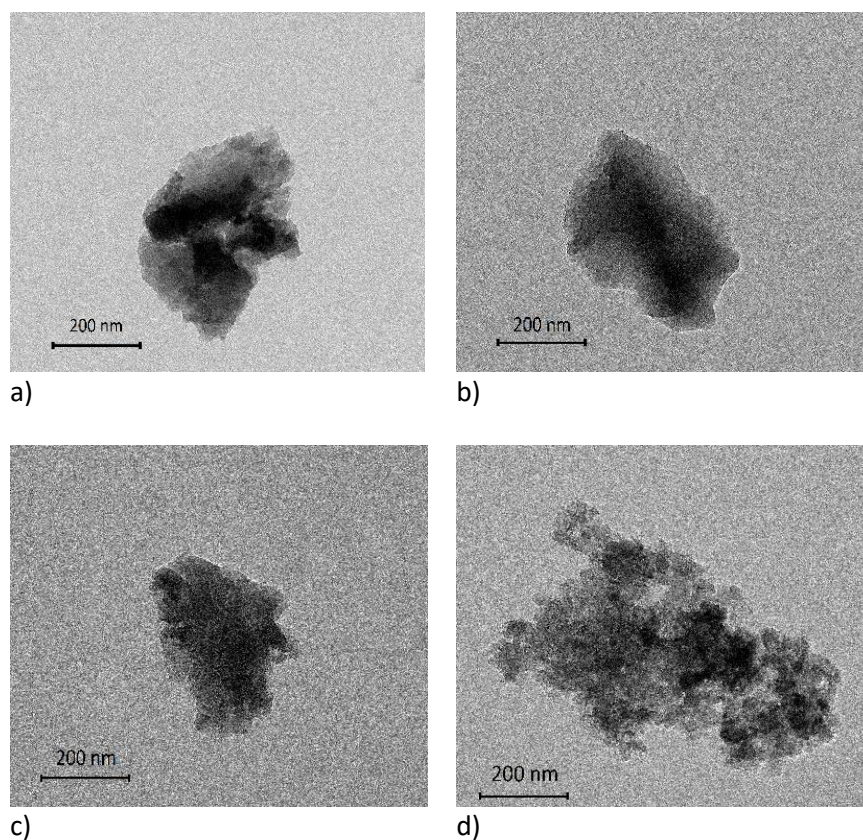


**Fig. 4.** TEM images of the activated peat samples. The magnification for a, b, and c is 100 kX, and for d is 200 kX; a) P<sub>1\_873</sub>; b) P<sub>½\_873</sub>; c) P<sub>¼\_873</sub>; d) P<sub>2\_873</sub>

## CONCLUSIONS

1. The yield of activated carbon varied according to the impregnation ratio and activation temperature used.
2. The carbon content increased with an increasing activation temperature.
3. The specific surface area and pore volume increased with increasing temperature and an impregnation ratio of up to 1. However, higher impregnation ratios caused a decrease for both parameters.
4. The pore size distribution was remarkably changed from micro- to mesoporous when the impregnation ratio was increased from ¼ to 2.
5. In order to achieve proper adsorption of MB and OII, pore volumes higher than 0.3 cm<sup>3</sup>/g were needed.
6. Finally, a slightly higher removal of OII compared with MB was observed.

## ACKNOWLEDGEMENTS

Toni Varila acknowledges the Bioraff Botnia foundation (21000030171 Interreg Botnia-Atlantica), Henrik Romar acknowledges the RenePro foundation (20200224 Interreg Nord), and Davide Bergna acknowledges the Central Ostrobothnia Cultural Foundation for personal grants. Facilities in the Nanocentre at the University of Oulu were used.

## REFERENCES CITED

- Ahmadpour, A., and Do, D. D. (1996). "The preparation of active carbons from coal by chemical and physical activation," *Carbon* 34(4), 471-479. DOI: 10.1016/0008-6223(95)00204-9
- Ahmedna, M., Marshall, W. E., and Rao, R. M. (2000). "Production of granular activated carbons from select agricultural by-products and evaluation of their physical, chemical and adsorption properties," *Bioresource Technol.* 71(2), 113-123. DOI: 10.1016/S0960-8524(99)00070-X
- Antal, M. J., and Grønli, M. (2003). "The art, science, and technology of charcoal production," *Ind. Eng. Chem. Res.* 42(8), 1619-1640. DOI: 10.1021/ie0207919
- Baçaoui, A., Yaacoubi, A., Dahbi, A., Bennouna, C., Luu, R. P. T., Maldonado-Hodar, F. J., Rivera-Utrilla, J., and Moreno-Castilla, C. (2001). "Optimization of conditions for the preparation of activated carbons from olive-waste cakes," *Carbon* 39(3), 425-432. DOI: 10.1016/S0008-6223(00)00135-4
- Barrett, E. P., Joyner, L. G., and Halenda, P. P. (1951). "The determination of pore volume and area distributions in porous substances. I. Computations from nitrogen isotherms," *J. Am. Chem. Soc.* 73(1), 373-380. DOI: 10.1021/ja01145a126
- Benaddi, H., Legras, D., Rouzaud, J., and Beguin, F. (1998). "Influence of the atmosphere in the chemical activation of wood by phosphoric acid," *Carbon* 36(3), 306-309. DOI: 10.1016/S0008-6223(98)80123-1
- Bouchemal, N., Belhachemi, M., Merzougui, Z., and Addoun, F. (2009). "The effect of temperature and impregnation ratio on the active carbon porosity," *Desalination and Water Treatment* 10(1-3), 115-120. DOI: 10.5004/dwt.2009.828
- Brunauer, S., Emmett, P. H., and Teller, E. (1938). "Adsorption of gases in multimolecular layers," *J. Am. Chem. Soc.* 60(2), 309-319. DOI: 10.1021/ja01269a023
- Caglayan, B., and Aksoylu, A. (2013). "CO<sub>2</sub> adsorption on chemically modified activated carbon," *J. Hazard. Mater.* 252-253, 19-28. DOI: 10.1016/j.jhazmat.2013.02.028
- Cox, M., Pichugin, A. A., El-Shafey, E. I., and Appleton, Q. (2005). "Sorption of precious metals onto chemically prepared carbon from flax shive," *Hydrometallurgy* 78(1-2), 137-144. DOI: 10.1016/j.hydromet.2004.12.006
- Demiral, H., Demiral, İ., Tümsük, F., and Karabacakoglu, B. (2008). "Pore structure of activated carbon prepared from hazelnut bagasse by chemical activation," *Surf. Interface Anal.* 40(3-4), 616-619. DOI: 10.1002/sia.2631
- Fu, T., and Li, Z. (2015). "Review of recent development in Co-based catalysts supported

- on carbon materials for Fischer-Tropsch synthesis,” *Chem. Eng. Sci.* 135, 3-20. DOI: 10.1016/j.ces.2015.03.007
- Hanna, F., Jan, K., and Marek, K. (2015). “Preparation and characterization of activated carbons from biomass material – giant knotweed (*Reynoutria sachalinensis*),” *Open Chemistry* 13(1), 1150-1156. DOI: 10.1515/chem-2015-0128
- Hayashi, J., Watkinson, A., Teo, K., Takemoto, S., and Muroyama, K. (1995). “Production of activated carbon from Canadian coal by chemical activation,” in: *8th International Conference on Coal Science*, Oviedo, Spain, pp. 1121-1124.
- Hirata, M., Kawasaki, N., Nakamura, T., Matsumoto, K., Kabayama, M., Tamura, T., and Tanada, S. (2002). “Adsorption of dyes onto carbonaceous materials from coffee grounds by microwave treatment,” *J. Colloid Interf. Sci.* 254(1), 17-22. DOI: 10.1006/jcis.2002.8570
- Khadiran, T., Hussein, M., Zainal, Z., and Rusli, R. (2015). “Textural and chemical properties of activated carbon prepared from tropical peat soil by chemical activation method,” *BioResources* 10(1), 986-1007. DOI: 10.15376/biores.10.1.986-1007
- Kumar, A., and Jena, H. M. (2015). “High surface area microporous activated carbons prepared from fox nut (*Euryale ferox*) shell by zinc chloride activation,” *Appl. Surf. Sci.* 356, 753-761. DOI: 10.1016/j.apsusc.2015.08.074
- Kumar, A., and Jena, H. M. (2016a). “Removal of methylene blue and phenol onto prepared activated carbon from fox nutshell by chemical activation in batch and fixed-bed column,” *Journal of Cleaner Production* 137, 1246-1259. DOI: 10.1016/j.jclepro.2016.07.177
- Kumar, A., and Jena, H. M. (2016b). “Preparation and characterization of high surface area activated carbon from fox nut (*Euryale ferox*) shell by chemical activation with  $H_3PO_4$ ,” *Results in Physics* 6, 651-658. DOI: 10.1016/j.rinp.2016.09.012
- Li, S., Pasc, A., Fierro, V., and Celzard, A. (2016). “Hollow carbon spheres, synthesis and applications - A review,” *J. Mater. Chem. A* 4(33), 12686–12713. DOI: 10.1039/C6TA03802F
- Lillo-Ródenas, M.A., Juan-Juan, J., Cazorla-Amorós, D., and Linares-Solano, A. (2004). “About reactions occurring during chemical activation with hydroxides,” *Carbon* 42(7), 1371-1375. DOI: 10.1016/j.carbon.2004.01.008
- Lillo-Ródenas, M. A., Cazorla-Amorós, D., and Linares-Solano, A. (2003). “Understanding chemical reactions between carbons and NaOH and KOH: An insight into the chemical activation mechanism,” *Carbon* 41(2), 267-275. DOI: 10.1016/S0008-6223(02)00279-8
- Liu, T.-H. (2010). “Development of mesoporous structure and high adsorption capacity of biomass-based activated carbon by phosphoric acid and zinc chloride activation,” *Chem. Eng. J.* 158(2), 129-142. DOI: 10.1016/j.cej.2009.12.016
- Liu, Z., Huang, Y., and Zhao, G. (2016). “Preparation and characterization of activated carbon fibers from liquefied wood by  $ZnCl_2$  activation,” *BioResources* 11(2), 3178-3190. DOI: 10.15376/biores.11.2.3178-3190
- Lua, A. C., and Yang, T. (2004). “Effect of activation temperature on the textural and chemical properties of potassium hydroxide activated carbon prepared from pistachio-nut shell,” *J. Colloid Interf. Sci.* 274(2), 594-601. DOI:

- 10.1016/j.jcis.2003.10.001
- Ma, J. F., Huang, D. Q., Zou, J., Li, L. Y., Kong, Y., and Komarneni, S. (2015). "Adsorption of methylene blue and Orange II pollutants on activated carbon prepared from banana peel," *Journal of Porous Materials* 22(2), 301-31. DOI: 10.1007/s10934-014-9896-2
- Marsh, H., and Rodríguez-Reinoso, F. (2006). *Activated Carbon*, Elsevier Science Ltd., Oxford, UK.
- Mohammad-Khah, A., and Ansari, R. (2009). "Activated charcoal: Preparation, characterization and applications: A review article," *International Journal of ChemTech Research* 1(4), 859-864.
- Özdemir, M., Bolgaz, T., Saka, C., and Şahin, O. (2011). "Preparation and characterization of activated carbon from cotton stalks in a two-stage process," *J. Anal. Appl. Pyrol.* 92(1), 171-175. DOI: 10.1016/j.jaap.2011.05.010
- Ozdemir, I., Şahin, M, Orhan, R., and Erdem, M. (2014). "Preparation and characterization of activated carbon from grape stalk by zinc chloride activation," *Fuel Process. Technol.* 125, 200-206. DOI: 10.1016/j.fuproc.2014.04.002
- Patrick, J. W. (1995). *Porosity in Carbons: Characterization and Applications*, Wiley, London, UK.
- Peng, X., Huang, D., Odoom-Wubah, T., Fu, D., Huang, J., and Qin, Q. (2014). "Adsorption of anionic and cationic dyes on ferromagnetic ordered mesoporous carbon from aqueous solution: Equilibrium, thermodynamic and kinetics," *J. Colloid Interf. Sci.* 430, 272-282. DOI: 10.1016/j.jcis.2014.05.035
- Qian, Q., Machida, M., and Tatsumoto, H. (2007). "Preparation of activated carbons from cattle-manure compost by zinc chloride activation," *Bioresource Technol.* 98(2), 353-360. DOI: 10.1016/j.biortech.2005.12.023
- Raposo, F., De La Rubia, M. A., and Borja, R. (2009). "Methylene blue number as useful indicator to evaluate the adsorptive capacity of granular activated carbon in batch mode: Influence of adsorbate/adsorbent mass ratio and particle size," *J. Hazard. Mater.* 165(1-3), 291-299. DOI: 10.1016/j.jhazmat.2008.09.106
- Rodríguez, A., García, J., Ovejero, G., and Mestanza, M. (2009). "Adsorption of anionic and cationic dyes on activated carbon from aqueous solutions: Equilibrium and kinetics," *J. Hazard. Mater.* 172(2-3), 1311-1320. DOI: 10.1016/j.jhazmat.2009.07.138
- Stimely, G., and Blankenhorn, P. (1985). "Effects of species, specimen size, and heating rate on char yield and fuel properties," *Wood Fiber Sci.* 17(4), 477-489.
- Teng, H., and Lin, H.-c. (1998). "Activated carbon production from low ash subbituminous coal with CO<sub>2</sub> activation," *AIChE J.* 44(5), 1170-1177. DOI: 10.1002/aic.690440514
- Yang, J., and Qiu, K. (2011). "Development of high surface area mesoporous activated carbons from herb residues," *Chem. Eng. J.* 167(1), 148-154. DOI: 10.1016/j.cej.2010.12.013
- Yang, K., Peng, J., Srinivasakannan, C., Zhang, L., Xia, H., and Duan, X. (2010). "Preparation of high surface area activated carbon from coconut shells using microwave heating," *Bioresource Technology* 101(15), 6163-6169. DOI:

doi.org/10.1016/j.biortech.2010.03.001

Yorgun, S., and Yıldız, D. (2015). "Preparation and characterization of activated carbons from Paulownia wood by chemical activation with H<sub>3</sub>PO<sub>4</sub>," *Journal of the Taiwan Institute of Chemical Engineers* 53, 122-131. DOI: 10.1016/j.jtice.2015.02.032

Yorgun, S., Vural, N., and Demiral, H. (2009). "Preparation of high-surface area activated carbons from Paulownia wood by ZnCl<sub>2</sub> activation," *Microporous and Mesoporous Materials* 122(1), 189-194. DOI:10.1016/j.micromeso.2009.02.032

Article submitted: June 9, 2017; Peer review completed: September 3, 2017; Revised version received and accepted: September 11, 2017; Published: September 15, 2017.  
DOI: 10.15376/biores.12.4.8078-8092